Desalination and Water Treatment
www.deswater.com

doi: 10.1080/19443994.2012.744950

51 (2013) 4719–4728
June

Taylor & Francis
Taylor & Francis Group

Kinetic evaluation and modeling for batch degradation of 2-hydroxybiphenyl and 2,2′-dihydroxybiphenyl by *Corynebacterium variabilis* Sh42

Samiha F. Deriase, Sherif A. Younis, Nour Sh. El-Gendy*

Egyptian Petroleum Research Institute, Nasr City, Cairo, Egypt
Email: nourepri@yahoo.com

Received 14 September 2012; Accepted 26 October 2012

ABSTRACT

This study evaluated the biodegradation kinetics of 2-hydroxybiphenyl (2-HBP) and 2,2′-dihydroxybiphenyl (2,2′-DHBP) with different initial concentrations range S_0 (5–50 mg/L) using suspended cultures of *Corynebacterium variabilis* Sh42 with fixed initial biomass concentration X_0 (315.8 mg/L) in a series of batch experiments. The cultures followed substrate inhibition kinetics. By fitting specific growth rates μ (h^{-1}) on suitable substrate inhibition models, biokinetic constants that are necessary to understand the kinetics of biodegradation process were evaluated by POLYMATH 6.1 software. Although Haldane and Yano and Koga (2) biokinetic equations for substrate inhibition seem to be the best adequate expressions for specific growth rates on 2-HBP and 2,2′-DHBP, respectively, an evident disagreement was observed between experimental and simulated profiles for bacterial growth X (mg/L) and substrate concentration S (mg/L). Correlation and simulation studies using a new proposed model based on modified Haldane equation gave better results.

Keywords: *Corynebacterium variabilis*; Biodegradation; 2-Hydroxybiphenyl; 2,2′-Dihydroxybiphenyl; Kinetics; Modeling

1. Introduction

The toxicity of hyroxybiphenyls and substituted hyroxybiphenyls has been exploited for many years in antimicrobial preparations used as biocides for industrial and agricultural purposes. The 2-Hydroxybiphenyl (2-HBP) has been widely used in disinfectant and preservative formulations, as an intermediate in the synthesis of dyes, resins, and rubber [1] and as a fungicide to control postharvest diseases of various fruits [2]. Hydroxylated biphenyls (HBPs) appear as major by-products of the industrial synthesis of phenol and dumping of the by-products on the production sites leads to groundwater and surface water contamination with HBPs at nearby location [1]. With the progress of understanding the biological degradation pathways of persistent pollutants, it becomes clear that HBPs are key intermediates produced from multiple sources. For example, they are produced from microbial metabolism of biphenyl, dibenzofuran, fluorene, and carbazole [3]. Metabolism of many polycyclic aromatic compounds (PACs) is blocked at some stage, and accumulation of intermediates, especially mono, di, and trihyroxbiphenyl, has been reported [4]. Furthermore, many reports have shown that plants metabolize major environmental contaminants, such as polychlorinated biphenyls (PCBs), to generate hydroxylated derivatives [5,6].

*Corresponding author.

Microbial degradation of 2-HBP and 2,2′-dihydroxybiphenyl (2,2′-DHBP) has become important to researchers involved in the desulfurization of coal and petroleum, since they are reported to be the end products of the microbial desulfurization of dibenzothiophene (DBT), a major sulfur-containing component of fossil fuel [7–11]. Some previous studies have indicated that final metabolite 2-HBP or 2,2′-DHBP of DBT biodegradation via 4S pathway could inhibit the microbial growth and DBT biodegradation [8,12]. The 2-HBP and 2,2′-DHBP produced through 4S-pathway are reported to be further metabolized to benzoic acid and salicylic acid, respectively, in complete mineralization pathway [13,14].

HBPs are by-products which have been identified as contaminants in almost every component of the global ecosystem and they constitute a severe environmental hazard because of their high toxicity. The concern about persistence of HBPs in the environment is the driving force for studies aimed at elucidating their bacterial metabolism and environmental fate. Few studies report that bacterial strains are able to use HBPs as sole carbon and energy sources. *Pseudomonas azelaica* HB1 [15,16], *Comamonas testosteroni* B-356 [17] and *Corynebacterium variabilis* Sh42 [14] degrade 2-HBP and 2,2′-DHBP through a *meta*-clevage pathway.

Mathematical modeling is helpful for understanding the behavior of biological processes and predicting the substrate concentration in the system. Many studies have been investigated on the kinetic modeling for the biodegradation of phenols [18–25] and catechols [26–28]. So far, to the best of our knowledge, no reports have been published on the kinetic modeling for the biodegradation of HBPs.

In this study, growth and biodegradation kinetics for *C. variabilis* Sh42 on different initial concentrations S_0 (5–50 mg/L) range of 2-HBP and 2,2′-DHBP in batch systems were investigated. This work was also aimed to fit different substrate inhibition models for the studied initial concentration range of HBPs, to determine the corresponding biokinetic parameters, and to compare the goodness of fit for these models to estimate the best-fit one. Mathematical expressions, for modeling and simulating substrate (S mg/L) and biomass (X mg/L) concentration profiles throughout the time span of the batch experiments, were also proposed and successfully applied.

2. Materials and methods

2.1. Chemicals

The 2-HBP and 2,2′-DHBP were purchased from Sigma Chemical Company, USA. Acetonitrile (Ace) and water (W) used for high-performance liquid chromatography (HPLC) analysis were of HPLC grade and purchased from Aldrich. All other chemicals employed in this study were of analytical grade.

2.2. Micro-organism

Bacterial strain, *C. variabilis* Sh42, used in this study was previously isolated from hydrocarbon-polluted water sample collected from El-Lessan Area of Damietta River Nile Branch in Egypt for its ability to degrade different PACs [14].

2.3. Media

Luria-Bertani (LB) medium used for obtaining biomass was prepared according to Caro et al. [29].

Basal salts medium (BSM) with salinity value 3.1% used for degradation studies was prepared according to Piddington et al. [30].

2.4. Culture preparation

Cells were incubated at 30°C in LB broth medium for 24 h in a shaking incubator (150 rpm). Cells were harvested by centrifugation at 5,000 rpm for 15 min, then washed twice and re-suspended in BSM free of any C-source for inoculation.

2.5. Kinetic experiments

Two series of four batch experiments were conducted in 250 mL Erlenmeyer flasks containing 100 mL BSM and 5 mL of cell suspension (A_{600} 0.2, approximately equivalent to initial biomass concentration of X_0 315.8 mg/L). The initial pH was adjusted to 7. A stock solution (75 mg/L) of each of the studied HBPs was prepared in ethyl ether, diluted according to the required studied concentrations, and added individually under aseptic conditions to sterile BSM in a final concentration (5–50 mg/L). All experiments were carried out for a period of 7d in an orbital shaking incubator set at 150 rpm and 30°C. During the batch experiments, samples were collected from each flasks at designated time intervals to follow up change in pH, bacterial growth, and 2-HBP and 2,2′-DHBP removal. Specific growth rate μ (h^{-1}) was calculated from a semi-natural logarithm plot of biomass concentration vs. time in exponential phase for each initial substrate concentration.

2.6. Mathematical modeling

2.6.1. Determination of kinetic parameters

Growth kinetics is an essential and mandatory input for the design of any biological reactor, where

microbial degradation is carried out. In order to represent the growth kinetics on the studied substrates (2-HBP and 2,2′-DHBP), the experimental results of specific growth rate μ (h^{-1}) variation with initial substrate concentration S_0 (mg/L) were fitted to eight biokinetic models, listed in Table 1. Biokinetic constants that are necessary to understand the kinetics of biodegradation process were estimated from the obtained experimental results, using non-linear least square algorithm provided by POLYMATH 6.1 software package.

2.6.2. Conventional modeling of cell growth and substrate biodegradation kinetics

For batch biodegradation process, the following differential equations (derived from mass-balance considerations) are often used for describing both biomass growth (X mg/L) and substrate (S mg/L) consumption, when cell decay and intermediates produced during the batch process are negligible [18].

Change in cell concentration can be described by:

$$\frac{dX}{dt} = \mu X \quad (1)$$

Change in substrate concentration can be defined by:

$$\frac{dS}{dt} = -qX \quad (2)$$

where q (h^{-1}) is the specific substrate degradation rate.

The relation between q (h^{-1}) and μ (h^{-1}) can be approximately expressed by:

$$q = \frac{\mu}{Y_{X/S}} \quad (3)$$

The relationship between biomass formation and substrate consumption can be approximately determined by the yield coefficient:

$$Y_{X/S} = -\frac{dX/dt}{dS/dt} = -\frac{dX}{dS} = -\frac{X - X_0}{S - S_0} \quad (4)$$

In order to estimate the cell growth and substrate biodegradation profiles, simulating the dynamic model given by Eqs. (1)–(4) together with the best fit biokinetic model equation describing the dependence of specific growth rate μ (h^{-1}) on the concentration of each substrate (S mg/L) was done using Runge–Kutta–Fehlberg algorithm for numerical integration of the ordinary differential equations provided by POLYMATH 6.1 software.

2.7. Analytical techniques

Bacterial growth was monitored by optical density O.D. (A_{600}) using UV/Vis spectrophotometer (UNICAM, model 8625) and non-inoculated BSM was used as blank. The cell concentration was also calculated

Table 1
Biokinetic parameters obtained by different models

Model	Substrate	Parameters	R^2	RMSE
Aiba $\mu = \mu_{max}\frac{Se^{(-S/K_i)}}{K_s+S}$ [31]	2-HBP	$\mu_{max} = 0.044$, $K_s = 0.860$, $K_i = 102$	0.995	3×10^{-4}
	2,2′-DHBP	$\mu_{max} = 0.051$, $K_s = 1.520$, $K_i = 102$	0.994	1×10^{-4}
Haldane $\mu = \frac{\mu_{max}S}{K_s+S+(S^2/K_i)}$ [32]	2-HBP	$\mu_{max} = 0.045$, $K_s = 0.894$, $K_i = 85.45$	1.000	6×10^{-5}
	2,2′-DHBP	$\mu_{max} = 0.053$, $K_s = 1.880$, $K_i = 69.69$	0.989	2×10^{-4}
Monod $\mu = \frac{\mu_{max}S}{K_s+S}$ [33]	2-HBP	$\mu_{max} = 0.032$, $K_s = 1.948$	0.859	2×10^{-3}
	2,2′-DHBP	$\mu_{max} = 0.034$, $K_s = 0.563$	0.203	2×10^{-3}
Moser $\mu = \frac{\mu_{max}S^n}{K_s+S^n}$ [34]	2-HBP	$\mu_{max} = 0.089$, $K_s = 0.368$, $n = -0.443$	0.999	1×10^{-4}
	2,2′-DHBP	$\mu_{max} = 0.038$, $K_s = 1.4\text{x}10^{-8}$, $n = -4.301$	0.787	3×10^{-4}
Teissier $\mu = \mu_{max}(e^{(-S/K_i)} - e^{(-S/K_s)})$ [35]	2-HBP	$\mu_{max} = 0.051$, $K_s = 0.165$, $K_i = 76.32$	0.929	1×10^{-3}
	2,2′-DHBP	$\mu_{max} = 0.044$, $K_s = 2.471$, $K_i = 134$	0.968	3×10^{-4}
Webb $\mu = \mu_{max}\frac{S(1+S/K)}{K_s+S+S^2/K_i}$ [35]	2-HBP	$\mu_{max} = 0.088$, $K_s = 1.203$, $K_i = 21.36$, $K = 5.523$	0.993	3×10^{-4}
	2,2′-DHBP	$\mu_{max} = 0.062$, $K_s = 2.891$, $K_i = 102$, $K = 25.45$	0.963	3×10^{-4}
Yano and Koga 1 $\mu = \frac{\mu_{max}S}{S+K_s+(S^2/K_1)+(S^2/K_2^2)}$ [36]	2-HBP	$\mu_{max} = 0.089$, $K_s = 2.164$, $K_1 = 14.16$, $K_2 = 7.6 \times 10^4$	0.598	3×10^{-3}
	2,2′-DHBP	$\mu_{max} = 0.087$, $K_s = 6.049$, $K_1 = 22.06$, $K_2 = 1 \times 10^4$	0.390	1×10^{-3}
Yano and Koga 2 $\mu = \frac{\mu_{max}S}{S+K_s+(S^3/K^2)}$ [36]	2-HBP	$\mu_{max} = 0.038$, $K_s = 1.320$, $K = 83.35$	0.993	3×10^{-4}
	2,2′-DHBP	$\mu_{max} = 0.043$, $K_s = 0.784$, $K = 77.33$	0.997	9×10^{-5}

from a predicted relationship between A_{600} and dry cell weight X (mg/L).

Liquid–liquid extraction for quantitative analysis of residual HBPs was carried out by using ethyl acetate as the extractant. After the extraction, ethyl acetate layer was analyzed using HPLC model Waters 600E equipped with a UV detector model Waters 2487 (set at 254 nm) and C18 reversed phase column (4.6×250 mm, 300 Å, 5μ). The mobile phase was Ace: W (40:60 v/v), flow rate was 1 mL/min, and injection volume was 2 μL. Standard curves were established for each of the studied compounds.

All experiments and measurements were done in duplicates and arithmetic averages were taken throughout the data analysis and calculations.

3. Results and discussion

Culture pH is reported to be important parameter in degradation process [20]. The monitored pH values in this study were between 7 and 6.5, and no pH adjustment was required. The relatively high content of mono- and di- basic phosphates in the BSM provided a good pH buffering capacity.

Loss due to abiotic process within the incubation period in control flasks was negligible for 2-HBP and 2,2′-DHBP (data not shown).

By investigating cell growth and HBPs degradation throughout the studied time span experiments, it was found that *C. variabilis* Sh42 expressed no lag phases in growth or biodegradation (BD) all over the studied concentration range. This indicates the well adaptation of Sh42 biodegrading enzymes towards the studied HBPs, although of their toxicity. This may be attributed to the previous isolation and enrichment of Sh42 on 2,2′-DHBP [14]. Time to reach stationary phase increased with increasing initial HBPs concentrations. For relatively low initial HBPs concentrations (5 and 10 mg/L), after the occurrence of the highest growth peaks at 36 h and 48 h for 2-HBP and 48 h and 60 h for 2,2′-DHBP, respectively, continuous decrease in biomass concentration was observed. The presence of toxic intermediate compounds, and/or the depletion of the HBPs (C-source) required for growth, may be the reason for low sustainability of the micro-organism. While for relatively high initial HBPs concentrations (25 and 50 mg/L), maximum growth was occurred at 72 and 120 h for 2-HBP and 108 and 144 h for 2,2′-DHBP, respectively, and remained nearly sustained till the end of incubation period. The maximum biomass yields of these bioprocesses were also found to decline with increase in initial substrate concentration recording (277, 178, 153, and 59) and (316, 167, 149, and 56) for initial substrate concentration of 5, 10, 25, and 50 mg/L, 2-HBP and 2,2′-DHBP, respectively. This may be because more energy is required to overcome the effect of substrate inhibition at high concentrations of HBPs. In addition, the production and accumulation of various intermediates may be responsible for the decrease in cell mass yield [37]. In such a case, conventional approaches of modeling based on a constant biomass yield will not be valid if a single model was to be applicable over the entire studied concentration range of HBPs.

It was also observed that the BD efficiencies of *C. variabilis* Sh42 decreased with increase in initial substrate concentration. The majority of biodegradation took place during exponential phase. For 2-HBP, complete removal of 5 and 10 mg/L was achieved after 48 and 96 h, respectively, while 91 and 83% removal occurred after 168 h at S_0 25 and 50 mg/L. Rate of degradation of 2,2′-DHBP was less than that of 2-HBP, where complete removal of 5 and 10 m/L was achieved after 96 and 108 h while 92 and 86% removal was achieved after 168 h at S_0 25 and 50 mg/L, respectively. There is an obvious time lag between reaching maximum growth and maximum degradation. This could be attributed to the biodegradation process itself, which might produce toxic metabolites to the cells and/or intermediates on which growth occurred instead of the initial substrate.

3.1. Determination of kinetic growth parameters

In order to optimize the concentration range of each studied compound for which the exponential growth rate of *C. variabilis* Sh42 is the highest. The specific growth rates (μ, h^{-1}) corresponding to each studied concentration of 2-HBP and 2,2′-DHBP were determined and fitted in the eight substrate inhibition models listed in Table 1. The variation of experimental μ (h^{-1}) as a function of initial HBPs concentrations S_0 (mg/L) and the fitted curves, by applying the eight biokinetic models, is represented in Figs. 1 and 2 for 2-HBP and 2,2′-DHBP, respectively.

Results, as represented in Figs. 1 and 2, revealed that, Sh42 exhibited an increasingly inhibitory response to the substrate initial concentrations. The specific growth rate of Sh42 reached its maximum at S_0 of 5 mg/L and 10 mg/L for 2-HBP and 2,2′-DHBP, respectively. After which sharp decline occurred in case of 2-HBP and gradual one occurred in case of 2,2′-DHBP. This indicates the intense toxicity of the studied HBPs.

Absolute values of the optimized kinetic parameters for various models along with both correlation coefficient (R^2) and root-mean-square error (RMSE) between experimental and predicted specific growth

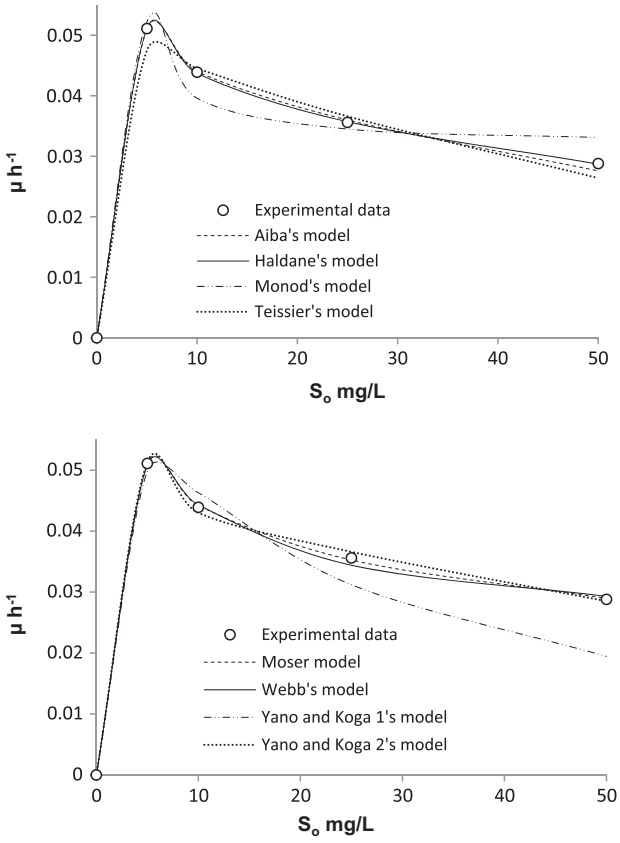

Fig. 1. Experimental (symbols) and predicted (lines) specific growth rates of *C. variabilis* Sh42 on 2-HBP.

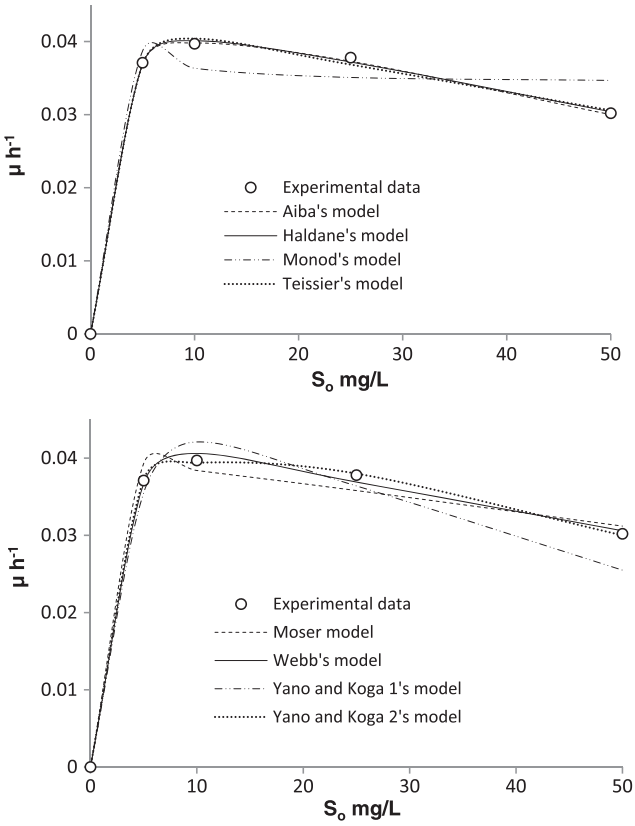

Fig. 2. Experimental (symbols) and predicted (lines) specific growth rates of *C. variabilis* Sh42 on 2,2´-DHBP.

rate values are listed in Table 1. Optimization of these biokinetic parameters are highly sensitive to their initial guess values required as input during regression analysis. Improper initial guess values may result in inaccurate values of the parameters, which in turn change the accuracy of simulated cell growth and substrate degradation profiles. Therefore, in this study sensitivity analysis for the estimation of these initial guess values was carried out.

From Figs. 1 and 2 and according to values of both R^2 and RMSE, it was observed that, between the eight different models, Haldane model for 2-HBP and Yano and Koga 2 model for 2,2´-DHBP provide best fit for experimental data with highest R^2 (1.0 and 0.997, respectively) and least RMSE value (6×10^{-5} and 9×10^{-5}, respectively). Accordingly, these models may be proposed as the kinetic models to describe the batch HBPs biodegradation behavior of *C. variabilis* Sh42.

To estimate the degree of toxicity of 2-HBP and 2,2´-DHBP on *C. variabilis* Sh42, Haldane model, the most widely used model, was applied. The two biokinetic constants are: K_i, the inhibition constant, is a measure of sensitivity by inhibitory substances and K_s, half-saturation constant, is defined as the substrate concentration at which μ equals to half μ_{max}. Since the studied HBPs expressed inhibitory effects on Sh42, thus according to Nuhoglu and Yalcin [18], if the substrate is inhibitory it is not possible to observe an actual μ_{max}. Thus, K_s could be taken on a hypothetical meaning. It can be shown that Haldane equation will go through maximal value $d_\mu/ds = 0$, at substrate concentrations S^* mg/L (for inhibitory substrates, it is the concentration at which the micro-organisms exhibited their maximum utilization rate, $S^* = \sqrt{K_s K_i}$), and the μ value corresponding to this concentration, $\mu^* = \frac{\mu_{max}}{2(\sqrt{K_s/K_i})+1}$. This reflects that the degree of inhibition is determined by K_s/K_i ratio and not just by K_i alone. The larger the K_s/K_i is, the smaller the μ^* (h^{-1}) relative to μ_{max}, and thus lower the degree of inhibition. From the results listed in Table 1, it can be concluded that, the maximum specific growth rate on 2,2´-DHBP (μ_{max} 0.053 h^{-1}) was greater than that of 2-HBP (μ_{max} 0.045 h^{-1}). Considering the fact that K_s (mg/L) is inversely proportional to the affinity of the microbial system for the substrate [38], Sh42 showed higher affinity to 2-HBP (K_s 0.894 mg/L) than that of 2,2´-DHBP (K_s 1.88 mg/L). The S^* for 2-HBP was

smaller than that of 2,2´-DHBP (8.21 and 11.45 mg/L, respectively). The Ks/K_i ratio of 2-HBP is smaller than that of 2,2´-DHBP (0.01 and 0.027, respectively) and the corresponding μ^* ($2.58x10^{-3}$ and $2.22x10^{-3}$, respectively). These data indicated that the toxicity and inhibition effects of 2-HBP on Sh42 are higher than those of 2,2´-DHBP.

3.2. Simulation with conventional models

The rate of substrate consumption is the most important measure of microbe performance. For modeling growth and substrate concentration change with time, simulating model described by Eqs. (1)–(4) with Haldane and Yano and Koga 2 biokinetic model equations for 2-HBP and 2,2´-DHBP (Table 1), respectively, was done. Simulations were performed for each studied initial HBPs concentration. Initial biomass concentration X_0 was 315.8 mg/L. The kinetic constants of

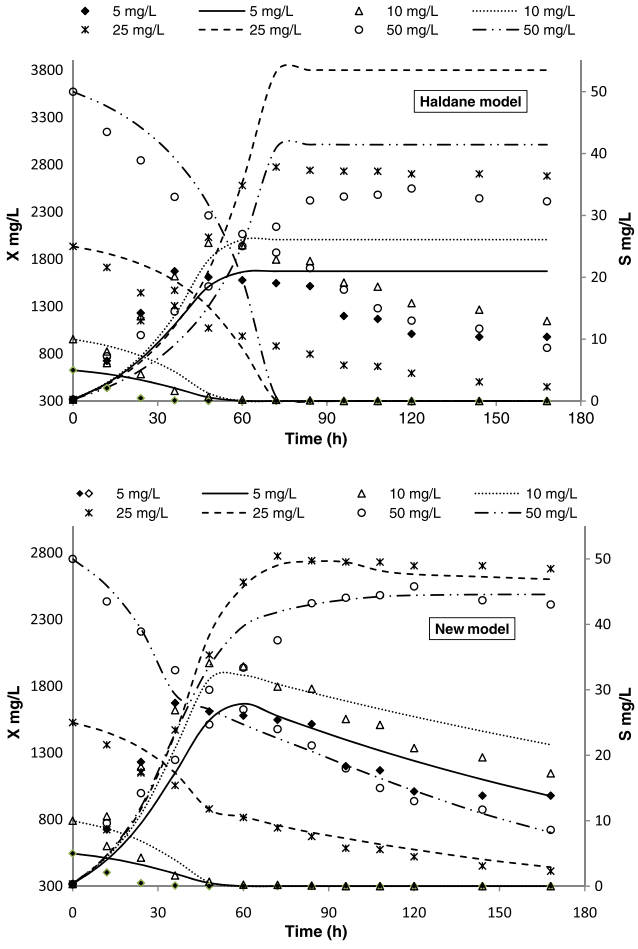

Fig. 3. Experimental (symbols) and simulated (lines) growth and biodegradation profiles of *C. variabilis* Sh42 on different initial concentrations of 2-HBP.

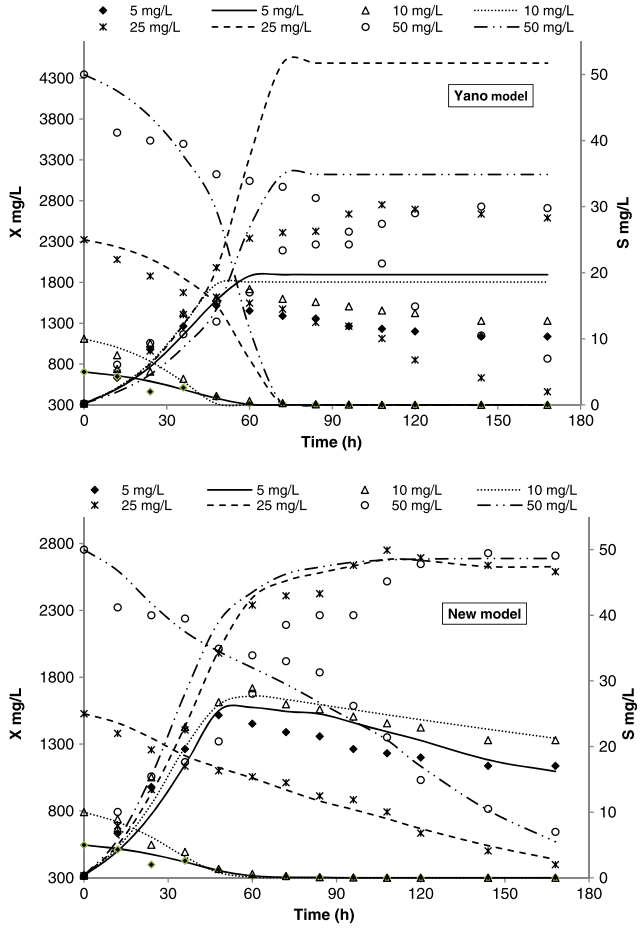

Fig. 4. Experimental (symbols) and simulated (lines) growth and biodegradation profiles of *C. variabilis* Sh42 on different initial concentrations of 2,2´-DHBP.

both Haldane and Yano and Koga 2 model equations used in simulations (μ_{max} 0.045 h^{-1}, K_s 0.894 mg/L, and K_i 85.45 mg/L) and (μ_{max} 0.043 h^{-1}, K_s 0.784 mg/L, and the positive constant K 77.33 mg/L), respectively, were those obtained from experimental data.

The change of measured and simulated biomass and HBPs concentrations with time is shown in Figs. 3 and 4. It is clearly seen from Fig. 3 that, although the Haldane biokinetic equation for substrate inhibition represents the best adequate expression for specific growth rate μ (h^{-1}) of Sh42 on 2-HBP, an evident disagreement was observed between measured and simulated profiles for cell growth and substrate degradation at different initial concentrations. But for 2,2´-DHBP, it is well observed from Fig. 4 that Yano and Koga 2 model is fairly adequate to reflect the growth and biodegradation profiles of Sh42 on relatively low initial 2,2´-DHBP concentration (5 and 10 mg/L). However, when S_0 higher than 10 mg/L was applied, the Yano and Koga 2 model has began

to fail. For S_0 25 and 50 mg/L, the Yano and Koga 2 predicted shorter complete degradation and higher bacterial growth than the measured ones.

This evident disagreement between measured and predicted profiles may be adjusted by using different sets of model parameters. But, it is appropriate to use one set of model parameters in any modeling effort. Accordingly, certain modification has been proposed by Nuhoglu and Yalcin [18] to overcome this disagreement between experimental and simulated profiles, by introducing cell decay rate coefficient b ($0.001\,h^{-1}$) into Eq. (1) and describing the change in cell concentration to be in the following form:

$$\frac{dX}{dt} = \mu X - bX \tag{5}$$

where value of b was obtained by trial and error method.

The established kinetic equations, Haldane and Yano and Koga 2 for 2-HBP and 2,2′-DHBP, respectively, were used to substitute specific growth rate μ (h^{-1}) in Eq. (5). Still an evident disagreement between measured and simulated profiles was observed with an average maximum percentage deviation of 22 and 44% for cell growth and 63 and 67% for substrate degradation, respectively.

3.3. Simulation with a new proposed model

Haldane equation has been used widely to describe cell growth kinetics on inhibitory substrates. This equation has been also often used for the prediction of substrate degradation rate by assuming a constant cell mass yield. It has been pointed out in the preceding discussion that the apparent yield coefficient for biomass is affected by initial HBPs concentrations. Additionally, during biodegradation of HBPs with *C. variabilis* Sh42, various metabolic intermediates are produced and accumulated [14]. Introducing the effect of these intermediates into the model equations would make the model complicated. Moreover, analytical determination of each intermediate would be difficult. However, assuming that the concentration of intermediates is proportional to the removal amount of substrate [18,37], therefore, the degraded amount of HBPs can be reasonably used to represent the concentration of intermediates. So, in order to consider the effect of these intermediates on HBPs degradations rate and to extend the model over a wide range of initial substrate concentrations, a new proposed model based on modified Haldane Eq. (7) describing the micro-organism concentration change is proposed. The new proposed mathematical model is described by the following equations:

Cell concentration change:

$$\frac{dX}{dt} = \mu X - b'X \tag{6}$$

By dividing the time span of the biodegradation process into subintervals, according to the assumption of the production and accumulation of metabolic intermediates during the process, the decay rate coefficient b' (h^{-1}) is changed for these subintervals according to logical IF statements included in the implemented computer program.

The q (h^{-1}) and μ (h^{-1}) are related to each other as represented previously in Eqs. (3) and (4), where μ (h^{-1}) is represented by modified Haldane equation:

$$\mu = \frac{\mu'_{max} S}{K'_s + S + f(i)} \tag{7}$$

where $f(i)$ represents the functional relationship of effect of metabolite intermediates on HBPs biodegradation process. The $f(i)$ is analogous to substrate inhibition term S^2/K_i in classical Haldane equation Table 1.

$f(i)$ is expressed as follows:

$$f(i) = \frac{(S_0 - S)^2}{K'_i} \tag{8}$$

These equations are coupled with Eq. (2), describing the change in HBPs concentration with time. Since, the kinetic model of Yano and Koga 2 has no substrate inhibition term (S^2/K_i), so, the new proposed model was applied for both 2-HBP and 2,2′-DHBP. This is due to the fact that Haldane equation takes care of the values of inhibition constant K_i, which is an important parameter in understanding the kinetics of the micro-organism in the system.

The resulted simulated profiles of the new proposed model for 2-HBP and 2,2′-DHBP are presented in Figs. 3 and 4, respectively. It is well observed that the evident disagreement between measured and simulated profiles for cell growth and substrate concentrations is overcome and adjusted by using model parameters obtained using non-linear regression algorithm available in POLYMATH 6.1 (μ'_{max} $0.041\,h^{-1}$, K'_s 1.06 mg/L, and K'_i 87.95 mg/L) and (μ'_{max} $0.054\,h^{-1}$, K'_s 4 mg/L, and K'_i 61.53 mg/L) for 2-HBP and 2,2′-DHBP, respectively. While adjusting the interactive changeable biomass decay rate coefficient b′, it was found to be in the range (0.0001–0.007 h^{-1}). The average maxi-

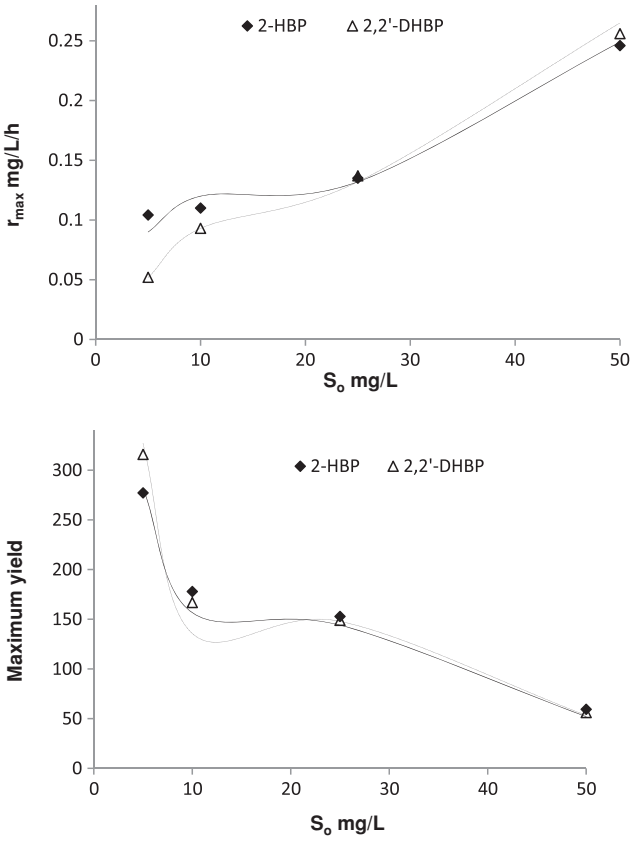

Fig. 5. Comparison between experimental (symbols) and calculated (lines) values of maximum degradation rate and yield.

mum percentage deviation reached 6.2 and 7.2% for cell growth and 11 and 10.2% for substrate degradation in the case of 2-HBP and 2,2′-DHBP, respectively. Fig. 5 represents the experimental and calculated values of maximum degradation rate (r_{max}, mg/L/h) and maximum biomass yield, which confirmed the adequacy of the new proposed model for estimating cell growth and degradation rates of *C. variabilis* Sh42 on the studied concentration range (5–50 mg/L) of HBPs.

4. Conclusions

C. variabilis Sh42 can utilize 2-HBP and 2,2′-DHBP as sole carbon source over the studied range of initial concentrations (S_0 5–50 mg/L). The growth kinetics of *C. variabilis* Sh42 does not follow a simple Monod's kinetics. Substrate inhibition is exhibited in batch experiments. By fitting specific growth rates μ (h^{-1}) on eight substrate inhibition models, biokinetic constants that are necessary to understand the kinetics of biodegradation process were evaluated, which confirmed good tolerance, growth, and degradation capabilities of Sh42 on the studied concentration ranges of 2-HBP and 2,2′-DHBP. Although, Haldane model for 2-HBP and Yano and Koga 2 model for 2,2′-DHBP provide best fit for experimental data of specific growth rate μ (h^{-1}) with highest R^2 (1.0 and 0.997, respectively) and least RMSE value (6×10^{-5} and 9×10^{-5}, respectively). An evident disagreement was observed between experimental and simulated profiles for bacterial growth X (mg/L) and substrate concentration S (mg/L). By introducing a constant cell decay rate coefficient b (0.001 h^{-1}), still an evident disagreement between measured and simulated profiles was observed with average maximum percentage deviation of 22 and 44% for cell growth and 63 and 67% for substrate degradation, respectively.

From the quantitative discussion of modeling relationship between cell growth rate and substrate consumption rate, it was found that the direct coupling of substrate consumption rate with the cell growth model is warranted only under certain conditions (e.g. constant cell yield). However, for HBPs degradation over a wide range of initial substrate concentrations, the cell mass yield was found to vary. Variations of the biomass decay rate coefficient during the time course of batch experiment were found to exert a great influence on biodegradation process, with the assumption of existence of some metabolic intermediates that would exert some inhibition on HBPs degradation. Correlation and simulation studies using a new proposed model based on modified Haldane equation were established and these factors were taken into consideration in the proposed HBPs degradation model. The proposed model is capable of describing growth and HBPs degradation profiles very well over the studied initial HBPs concentrations (5–50 mg/L). The average maximum percentage deviation reached 6.2 and 7.2% for cell growth and 11 and 10.2% for substrate degradation in the case of 2-HBP and 2,2′-DHBP, respectively.

The approaches of modeling and simulation for the experimental results obtained in this work are considered to be essential in order to facilitate understanding the biodegradation processes of contaminants under study for better achievement of biotreatment of contaminated sites and industrial effluents. Since biological treatments are preferred for large-scale removal of organic pollutants.

Further work is now undertaken in Egyptian Petroleum Research Institute Biotechnology Laboratory to determine and study the effect of intermediates produced during biodegradation processes of 2-HBP and 2,2′-DHBP, proposing new mathematical models that explicitly takes into account the change in metabolites and biomass concentrations throughout the time

span of the biodegradation processes over wide range of substrate concentration (5–500 mg/L).

List of symbols

b — biomass decay rate coefficient, h^{-1}
b' — interactive changeable biomass decay rate coefficient, h^{-1}
K — positive constants, mg/L
K_i — substrate inhibition constant, mg/L
K_s — substrate affinity constant, mg/L
n — empirical constant
q — specific degradation rate, h^{-1}
q_{max} — maximum specific degradation rate, h^{-1}
S — substrate concentration at time t, mg/L
S_0 — initial substrate concentration, mg/L
t — time, h
X — biomass concentration at time t, mg/L
X_0 — initial biomass concentration, mg/L
$Y_{X/S}$ — yield (g biomass/g substrate)
μ — specific growth rate, h^{-1}
μ_{max} — maximum specific growth rate, h^{-1}

References

[1] M.M. Jaspers, W.A. Suske, A. Schmid, D.A.M. Goslings, H.E. Kohler, J.R. Van Der Meer, HbpR, a new member of the XylR/DmpR subclass within the NtrC family of bacterial transcriptional activators, regulates epression of 2-hydroxybiphenyl metabolism in *Pseudomonas azelaica* HBP1, J. Bacteriol. 182(2) (2000) 405–417.

[2] J.W. Eckert, Control of postharvest diseases, in: M.R. Siegel, H.D. Sisler (Ed.), Antifungal Compounds, Marcel Dekker, New York, NY, 1977, vol. 1, pp. 269–352.

[3] H. Nojiri, T. Omori, Molecular bases of aerobic bacterial degradation of dioxins: Involvement of angular dioxygenation, Biosci. Biotechnol. Biochem. 66 (2002) 2001–2016.

[4] K. Furukawa, N. Tomizuka, A. Kamibayashi, Effect of chlorine substitution on the bacterial metabolism of various polychlorinated biphenyls, Appl. Environ. Microbiol. 38 (1979) 301–310.

[5] R.K. Puri, Q.P. Ye, S. Kapila, W.R. Lower, V. Puri, Plant uptake and metabolism of polychlorinated biphenyls (PCBs), in: W. Wang, J.W. Gorsuch, J.S. Hughcs (Eds.), Plants for Environmental Studies, CRC Press, Boca Raton, FL. 1997, pp. 481–513.

[6] L. Chroma, M. Moeder, P. Kucerova, T. Macek, M. Mackova, Plant enzymes in metabolism of polychlorinated biphenyls, Fresen. Environ. Bull. 12 (2003) 291–295.

[7] W.A. Suske, M. Held, A. Schmid, T. Fleischmann, M.G. Wubbolts, H.P.E. Kohler, Purification and characterization of 2-hydroxybiphenyl-3-monooxygenase, a novel NADH-dependent, FAD-containing aromatic hydroxylase from *Pseudomonas azelaica* HBP1, J. Biol. Chem. 272(39) (1997) 24257–24265.

[8] N.Sh. El-Gendy, L.A. Farahat, Y.M. Moustafa, N. Shaker, S.A. El-Temtamy, Biodesulfurization of crude and diesel oil by *Candida parapsilosis* NSh45 isolated from Egyptian hydrocarbon polluted sea water, Biosci. Biotechnol. Res. Asia 3(1) (2006) 5–16.

[9] H. Chen, W.J. Zhang, Y.B. Cai, Y. Zhang, W.C. Li, Elucidation of 2- hydroxybiphenyl effect on dibenzothiophene desulfurization by *Microbacterium* sp. strain ZD-M2, Bioresour. Technol. 9 (2008) 6928–6933.

[10] M. Ardakani, A. Amisefat, B. Rasekh, F. Yazdiyan, B. Zargar, M. Zarei, H. Najafzadeh, Biodesulfurization of dibenzothiophene by newly isolated, *Stenotrophomonas maltophilia* strain kho1, World Appl. Sci. J. 10(3) (2010) 272–278.

[11] G.A. Amin, Integrated two-stage process for biodesulfurization of model oil by vertical rotating immobilized cell reactor with the bacterium *Rodochoccus erythropolis*, J. Petrol. Environ. Biotechnol. 2(1) (2011) 1–4.

[12] M.K. Lee, J.D. Senius, M.J. Grossman, Sulfur-specific microbial desulfurization of sterically hindered analogs of dibenzothiophene, Appl. Environ. Microbiol. 61 (1995) 4362–4366.

[13] N.Sh. El-Gendy, Biodegradation potentials of dibenzothiophene by new bacteria isolated from hydrocarbon polluted soil in Egypt, Biosci. Biotechnol. Res. Asia 3(1) (2006) 95–106.

[14] N.Sh. El-Gendy, Y.M. Moustafa, S.A. Habib, Sh. Ali, Evaluation of *Corynebacterium variabilis* Sh42 as a degrader for different poly aromatic compounds, J. Am. Sci. 6(11) (2011) 343–356.

[15] H.P.E. Kohler, D. Kohler-Staub, D.D. Focht, Degradation of 2-hydroxybiphenyl and 2,2′-dihydroxybiphenyl by *Pseudomonas* sp. strain HBP1, Appl. Environ. Microbiol. 54 (1988) 2683–2688.

[16] H.P.E. Kohler, A. Schmid, M. van der Maarel, Metabolism of 2,2′-dihydroxybiphenyl by *Pseudomonas* sp. strainHBP1: Production and consumption of 2,2′,3-trihydroxybiphenyl, J. Bacteriol. 175 (1993) 1621–1628.

[17] M. Sondossi, D. Barriault, M. Sylvestre, Metabolism of 2,2′- and 3,3′-dihydroxybiphenyl by biphenyl catabolic pathway of *Comamonas testosteroni* B-356, Appl. Environ. Microbiol. 70(1) (2004) 174–181.

[18] A. Nuhoglu, B. Yalcin, Modelling of phenol removal in a batch reactor, Process Biochem. 40 (2005) 1233–1239.

[19] N.K. Sharma, L. Philip, S. Murty Bhallamudi, Aerobic degradation of phenolics and aromatic hydrocarbons in presence of cyanide, Bioresour. Technol. 121 (2012) 263–273.

[20] E. Sahinkaya, F.B. Dilek, Biodegradation kinetics of 2,4-dichlorophenol by acclimated mixed cultures, J. Biotechnol. 127 (2007) 716–726.

[21] S.E. Agarry, B.O. Solomon, T.O.K. Audu, Substrate utilization and inhibition kinetics: Batch degradation of phenol by indigenous monoculture of *Pseudomonas aeruginosa*, Int. J. Biotechnol. Mol. Biol. Res. 1(2) (2010) 22–30.

[22] A. Noworyta, A. Trusek-Holownia, S. Mielczarski, M. Kubasiewicz-Ponitka, An integrated pervaporation-biodegradation process of phenolic wastewater treatment, Desalination 198 (2006) 191–197.

[23] S.E. Agarry, B.O. Solomon, S.K. Layokun, Substrate inhibition kinetics of phenol degradation by binary mixed culture of *Pseudomonas aeruginosa* and *Pseudomonas fluorescence* from steady state and wash-out data, Afr. J. Biotechnol. 7(21) (2008) 3927–3933.

[24] K.V. Shetty, D.K. Verma, G. Srinikethan, Modelling and simulation of steady-state phenol degradation in a pulsed plate bioreactor with immobilized cells of *Nocardia hydrocarbonoxydans*, Bioprocess Biosyst. Eng. 34(1) (2011) 45–56.

[25] E.A. Wolski, I. Durruty, P.M. Haure, J.F. González, *Penicillium chrysogenum*: Phenol degradation abilities and kinetic model, Wat. Air Soil Pollut. 223(5) (2012) 2323–2332.

[26] A. Kumar, S. Kumar, Biodegradation kinetics of phenol and catechol using *Pseudomonas putida* MTCC 1194, Biochem. Eng. J. 22 (2005) 151–159.

[27] I. Stoilova, A. Krastanov, V. Stanchev, D. Daniel, M. Gerginova, Z. Alexieva, Biodegradation of high amounts of phenol, catechol, 2,4-dichlorophenol and 2,6-dimethoxyphenol by *Aspergillus awamori* cells, Enzyme Microb. Technol. 39(5) (2006) 1036–1041.

[28] M. Rigo, R.M. Alegre, J.R.M.V. Bezerra, N. Coelho, R.G. Bastos, Catechol biodegradation kinetics using *Candida parapsilopsis*, Brazilian Arch. Biol. Technol. 53(2) (2010) 481–486.

[29] A. Caro, K. Boltes, P. Leton, E. Garcia-Calvo, Biodesulfurization of dibenzothiophene by growing cells of *Pseudomonas putida* CECT5279 in biphasic media, Chemosphere 73 (2008) 663–669.
[30] C.S. Piddington, B.R. Kovacevich, T. Rambosek, Sequence and molecular characterization of a DNA region encoding the dibenzothiophene desulfurization operon of *Rhodococcus* sp. strain IGTS8, J. Appl. Environ. Microbiol. 61(2) (1995) 468–475.
[31] S. Aiba, M. Shoda, M. Nagatami, Kinetics of product inhibition in alcohol fermentation, Biotechnol. Bioeng. 10 (1968) 845–864.
[32] J.F. Andrews, A mathematical model for the continuous culture of microorganisms utilizing inhibitory substances, Biotechnol. Bioeng. 10 (1968) 707–723.
[33] J. Monod, The growth of bacterial cultures, Ann. Rev. Microbiol. 3 (1949) 371–394.
[34] S.K. Layokun, E.F. Umoh, B.O. Solomon, A kinetic model for the degradation of dodecane by *P. fluorescens* isolated from the oil polluted area, Warri in Nigeria, J. Nsche. 16 (1987) 48–52.
[35] V.H. Edwards, The influence of high substrate concentrations on microbial kinetics, Biotechnol. Bioeng. 12 (1970) 679–712.
[36] T. Yano, S. Koga, Dynamic behavior of the chemostat subject to substrate inhibition, Biotechnol. Bioeng. 11 (1969) 139–153.
[37] S.J. Wang, K.C. Loh, Modeling the role of metabolic intermediates in kinetics of phenol biodegradation, Enzyme Microb. Technol. 25 (1999) 177–184.
[38] S.E. Agsrry, B.O. Solomon, Kinetics of batch microbial degradation of phenols by indigenous *Pseudomonas fluorescence*, Int. J. Environ. Sci. Tech. 5(2) (2008) 223–232.